doi:10.4149/207_150821N454

H19 serves as a diagnostic biomarker and up-regulation of H19 expression contributes to poor prognosis in patients with gastric cancer

J. S. CHEN[1,‡], Y. F. WANG[2,‡], X. Q. ZHANG[1], J. M. LV[1], Y. LI[1], X. X. LIU[3], T. P. XU[4,*]

[1]Department of Oncology, Yizheng People's Hospital, Yangzhou 211400, Jiangsu Province, People's Republic of China; [2]Department of Pathology, The First People's Hospital of Yangzhou, The Second Clinical Medical College, Yangzhou University, Yangzhou 225000, Jiangsu province, People's Republic of China; [3]Department of Gastrointestinal Surgery, Subei People's Hospital of Jiangsu Province, Yangzhou University, Yangzhou 225001, Jiangsu Province, People's Republic of China; [4]Department of Oncology, the First Affiliated Hospital of Nanjing Medical University, No. 300 Guangzhou Road, Nanjing 210029, Jiangsu Province, People's Republic of China

**Correspondence: tongpeng_xu_njmu@edu.cn*
‡Contributed equally to this work.

Received August 21, 2015 / Accepted October 14, 2015

Emerging evidences indicate that dysregulated long noncoding RNAs (lncRNAs) are implicated in cancer tumorigenesis and progression and might be used as diagnosis and prognosis biomarker, or potential therapeutic targets. LncRNA *H19* has been reported to be upregulated in diverse human cancers; however, its clinical significance in gastric cancer (GC) remains elusive. Expression levels of *H19* in 128 pairs of GC and adjacent normal tissues, GC cell lines and GC juices compared to their corresponding controls were detected by real-time quantitative polymerase chain reaction (qPCR) assay. A receiver operating characteristic (ROC) curve and Kaplan–Meier analysis were constructed to evaluate the diagnostic and prognostic values. Univariate and multivariate analysis were performed using the Cox proportional hazard analysis. *H19* expression was remarkably increased in GC tissues and cell lines compared with that in the normal control, and its up-regulation was significantly correlated to invasion depth ($P < 0.001$), advanced TNM stage ($P = 0.002$) and regional lymph nodes metastasis ($P < 0.001$) in GC. *H19* levels were robust in differentiating GC tissues from controls [area under the curve (AUC) = 0.697; 95% confidence interval (CI) = 0.636–0.752, p<0.01]. Kaplan–Meier analysis demonstrated that increased *H19* expression contributed to poor overall survival ($P = 0.017$) and disease-free survival ($P = 0.024$) of patients. A multivariate survival analysis also indicated that *H19* could be an independent prognostic marker. The levels of *H19* in gastric juice from gastric patients were significantly higher than those from normal subjects ($P = 0.034$). Furthermore, knockdown of *H19* expression by siRNA could inhibit cell migration and invasion in GC cells partly via regulating E-cadherin protein expression. *H19* might serve as a promising biomarker for early detection and prognosis prediction of GC.

Key words: H19, gastric cancer, clinical relevance, invasion

Gastric cancer (GC) is the fourth most common malignancy in the world and is the second most frequent cause of cancer-related deaths worldwide, with particularly high incidence in East Asia. [1, 2]. Although GC is curable if detected early, most patients are diagnosed in the advanced stage and have poor prognosis [3]. The clinical stage, based on the TNM classification system, at the time of diagnosis is currently the most important prognostic factor, and the molecular mechanism involved in progression and metastasis of GC remains unclear [4]. Thus, novel findings on diagnosis and prognosis factors for GC would be of great clinical relevance.

A majority of the human genome is made up of non-coding RNAs (ncRNAs), indicating that ncRNAs could play significant regulatory roles in complex organisms[5]. These non-coding regions are interspersed throughout genomic DNA. One subcategory of these transcripts, called long noncoding RNAs (lncRNAs), are widely defined as transcribed RNA molecules more than 200 nucleotides in length and lacking an open reading frame of significant length[6]. It is known that lncRNAs are widely transcribed in the genome, but our understanding of their functions is limited. Many studies have revealed that the deregulated expression of lncRNAs plays a functional role

in a variety of disease states [7, 8]. Functional lncRNAs can be used for cancer diagnosis and prognosis, and serve as potential therapeutic targets; thus, lncRNAs can be considered as a new diagnostic and therapeutic gold mine in cancer[9].

Recently, the functions of some of the lncRNAs have been reported as regulators in different tumors [10-12]. For example, *HOTAIR*, which is one of the few well-studied lncRNAs, plays a significant role in tumor progression by regulation of oncogene or tumor suppressor gene expression through binding to PRC2 [10]. In addition, metastasis-associated lung ade-nocarcinoma transcript 1 (*MALAT1*) facilitated renal cell carcinoma aggressive through Ezh2 and interacts with miR-205[13]. Recently, multiple lines of evidences link dysregulation of lncRNAs to GC, such as *HOTAIR*, *MALAT1*, maternally expressed gene 3 (MEG3) and growth arrest-specific 5 (GAS5) [14-16]. However, the function of most lncRNAs in GC and their clinical significance remain incompletely understood.

Table 1. Correlation between *H19* expression and clinicopathological characteristics of GC

Clinical parameter	*H19*		Chi-squared test P-value
	High No. cases (n=64)	Low No. cases (n=64)	
Age (years)			0.724
<50	31	33	
>50	33	31	
Gender			0.585
Male	41	38	
Female	23	26	
Location			0.814
Distal	26	24	
Middle	25	24	
Proximal	13	16	
Size			0.723
>5cm	35	33	
<5cm	29	31	
Histologic differentiation			0.286
Well	10	11	
Moderately	17	26	
Poorly	27	18	
Undifferentiated	10	9	
Invasion depth			<0.001*
T1	5	24	
T2	10	25	
T3	29	8	
T4	20	7	
TNM Stages			0.002*
I	8	19	
II	22	31	
III	32	13	
IV	2	1	
Lymphatic metastasis			0.051
Yes	35	24	
No	29	40	
Regional lymph nodes metastasis			<0.001*
PN0	29	40	
PN1	5	14	
PN2	19	5	
PN3	11	5	
Distant metastasis			0.500
Yes	2	1	
No	62	63	

*P < 0.05

H19, is a paternally imprinted gene and is locate on chromosome 11p15.5, which does not encode for protein but encodes for a 2.3 kb noncoding RNA [17]. In the human genome, *H19* gene is a member of a highly conserved cluster of imprinted genes, including paternally expressed insulin-like growth factor 2 (Igf2) and maternally expressed *H19*, both of which are regulated by the differentially methylated region (DMR) or the imprinting control region (ICR) located 4 kb upstream of the *H19* gene [18]. It is highly expressed in embryogenesis but is nearly completely downregulated in most tissues after birth[18]. Currently, several studies have shown that *H19* is overexpressed in tumors and functions as an oncogene gene [19-21]. Recent studies have showed that *H19* is upregulated in human gastric carcinomas [22, 23]. However, the overall clinical role of *H19* in GC has not yet been well characterized.

In this study, we found that *H19* expression was upregulated in GC tissues and cell lines. High expression of *H19* was associated with clinicopathological characteristics and poor prognosis in GC patients. We also determined its prognostic role in GC, which might dramatically improve the therapeutic strategy of GC.

Materials and methods

Cell lines. Human gastric adenocarcinoma cancer cell lines SGC7901, BGC823, MGC803, AGS and MKN45 and the normal gastric epithelium cell line (GES1) were obtained from the Chinese Academy of Sciences Committee on Type Culture Collection cell bank (Shanghai, China). MGC803, AGS and BGC823 cells were cultured in RPMI 1640; MKN45, GES1 and SGC7901 cells were cultured in DMEM (GIBCO-BRL) medium supplemented with 10% fetal bovine serum (FBS), 100 U/ml penicillin and 100 mg/ml streptomycin (Invitrogen, Carlsbad, CA, USA) at 37°C in 5% CO_2.

Tissue samples and clinical data collection. In this study, we analyzed 128 patients who underwent resection of the primary GC at Yizheng People's Hospital of Jiangsu Province and Subei People's Hospital of Jiangsu Province. The study was approved by the Ethics Committee on Human Research of Yizheng People's Hospital of Jiangsu Province and Subei People's Hospital of Jiangsu Province and written informed consent was obtained from all patients. The clinicopathological characteristics of the GC patients are summarized in Table 1. All patients with GC have been followed up at intervals of 1–2 months until September 2014, and the median follow-

up period was 36 months (range, 20–48 months). Follow-up studies included physical examination, laboratory analysis, and computed tomography if necessary. Overall survival (OS) was defined as the interval between the dates of surgery and death. Disease-free survival (DFS) was defined as the interval between the dates of surgery and recurrence; if recurrence was not diagnosed, patients were censored on the date of death or the last follow-up.

Gastric juices were collected from 56 subjects, including 33 patients with GC (mean age, 61.7 ± 10.2 years) and 23 cases with normal mucosa or minimal gastritis (mean age, 57.3 ± 15.8 years) between July 2012 and November 2013 in the Endoscopy Center of the Yicheng People's Hospital of Jiangsu Province. For each case, the diagnosis was confirmed by endoscopic examination followed by pathological diagnosis of biopsies. Cases with normal mucosa or minimal gastritis, which had no family history of GC, were treated as the controls. Gastric juice specimens were centrifuged at 2,000×g for 30 min at 4 °C to remove cell fragments and mucus. Then, the pH was measured using a glass electrode pH meter. Finally, the supernatants were stored at −80 °C until use. The study protocol was approved by the Ethics Committee of Yizheng People's Hospital of Jiangsu Province. All specimens were handled and made anonymous following the ethical and legal standards.

RNA preparation and quantitative real-time polymerase chain reaction (qPCR). Total RNAs were extracted from tumorous and adjacent normal tissues or cultured cells using Trizol reagent (Invitrogen) following the manufacturer's protocol. For gastric juice RNA extraction, 750 µl Trizol LS reagent (Invitrogen) was mixed with 250 µl gastric juice. After vortex mixing for 30 s and then standing for 5 min, 200 µl chloroform was added. The Trizol–chloroform mixture was vortex-mixed for 15 s and then centrifuged at 12,000×g for 15 min at 4 °C. The upper aqueous phase was transferred to a fresh tube. Finally, RNA was extracted following the manufacturer's instructions. Total RNA was quantified using a SmartSpec Plus spectrophotometer (Bio-Rad, Hercules, CA, USA). The A260/A280 ratio was used to evaluate RNA purity. Reverse transcription (RT) and qPCR kits (Takara, Dalian, China) were used to evaluate the expression of *H19* in tissue samples, cultured cells and gastric juice. The primers used for glyceraldehyde 3-phosphate dehy-drogenase (GAPDH) and *H19* were as follows: 5'-TACAACCACTGCACTACCTG-3' (sense) and 5'-TGTTGCTGTAGCCAAATTCGTT-3' (antisense) for GAPDH. The primer sequences were 5'-TACAACCACTGCACTACCTG-3' (sense) and 5'-TGGAATGCTTGAAGGCTGCT-3' (antisense) for *H19*. Real-time PCR was performed in triplicate, and the relative expression of *H19* was calculated using the comparative cycle threshold (CT) ($2^{-\Delta\Delta CT}$) method with glyceraldehyde-3-phosphate dehydrogenase (GAPDH) as the endogenous control to normalize the data.

Cell transfection. To generate *H19*-knockdown BGC823 and MGC803 cells, the target sequence for *H19* siRNA or scrambled siRNA that did not correspond to any human sequence was synthesized by Invitrogen. The sequence of *H19* siRNA was 5'-GCAAGAAGCGGGTCTGTTT-3', and the scrambled siRNA was 5'-UUCUCCGAACGUGUCACGUTT-3'. BGC823 and MGC803 cells were grown on six-well plates to confluency and transfected using Lipofectamine 2000 (Invitrogen) according to the manufacturer's instructions. At 48 h post-transfection, cells were harvested for Western blot analysis.

Cell migration and invasion assays. For the migration assays, at 48 h post-transfection, 5×10^4 cells in serum-free media were placed into the upper chamber of an insert (8-µm pore size; Millipore). For the invasion assays, 1×10^5 cells in serum-free medium were placed into the upper chamber of an insert coated with Matrigel (Sigma-Aldrich). Medium containing 10% fetal bovine serum (FBS) was added to the lower chamber. After incubation for 24 h, the cells remaining on the upper membrane were removed with cotton wool. Cells that had migrated or invaded through the membrane were stained with methanol and 0.1% crystal violet, imaged, and counted using an IX71 inverted microscope (Olympus, Tokyo, Japan). Experiments were independently repeated three times.

Western blot assay and antibodies. Cells protein lysates were separated by 10% sodium dodecyl sulfate-polyacrylamide gel electrophoresis (SDS-PAGE), transferred to 0.22-µm NC membranes (Sigma), and incubated with specific antibodies. ECL chromogenic substrate was used to visualize the bands and the intensity of the bands was quantified by densitometry (Quantity One software; Bio-Rad). GAPDH antibody was used as control, and antibodies (1:1000 dilution) against E-cadherin and N-cadherin were purchased from BD. Antibodies (1:1000 dilution) against vimentin were purchased from Cell Signaling Technology (MA, USA).

Statistical analysis. All statistical analyses were performed using SPSS 20.0 software (IBM, SPSS, Chicago, IL, USA). The significance of the differences between groups was estimated by the Student t-test, $\chi 2$ test, or Wilcoxon test, as appropriate. DFS and OS rates were calculated by the Kaplan–Meier method with the log-rank test applied for comparison. Survival data were evaluated using univariate and multivariate Cox proportional hazards models. Variables with a value of $P < 0.05$ in univariate analysis were used in subsequent multivariate analysis on the basis of Cox regression analyses. Receiver operating characteristic (ROC) curves were constructed to evaluate the diagnostic value of *H19* levels, by plotting sensitivity versus 100% specificity. Two-sided p-values were calculated, and a probability level of 0.05 was chosen for statistical significance.

Results

***H19* was upregulated in tissues and cell lines.** *H19* expression levels were investigated using quantitative polymerase chain reaction (qPCR) assays in GC cell lines, including MGC803, BGC823, MKN45, SGC7901, AGS and the normal gastric epithelium cell line GES1. A significant high *H19*

expression was found in SGC7901, BGC823, MGC803, AGS and MKN45 compared to GES-1 (Fig. 1A). *H19* expression were further detected in 128 paired GC samples and adjacent histologically normal tissues and the results showed that *H19* expression was significantly higher in tumor tissues compared with adjacent normal tissues, 76.6 percentage was over-expression and 23.4 percentage was under-expression ($P < 0.01$; Fig. 1B).

***H19* expression and clinicopathological factors in GC.** To assess the correlation of *H19* expression with clinicopathological data, *H19* expression levels in tumor tissues were categorized as low or high in relation to the median value of relative *H19* expression (4.47-fold, tumors/noncancerous). Clinicopathological factors were analyzed in the high and low *H19* expression groups. As shown in Table 1, the high *H19* group (n = 64) showed higher invasion depth ($P < 0.001$), advanced TNM stage ($P = 0.002$) and regional lymph nodes metastasis ($P < 0.001$) than the lower *H19* expression group (n = 64). However, there was no significant correlation between *H19* expression and other clinicopathological features, such as age, gender, tumor location, tumor size, histologic grade, lymphatic metastasis, and distant metastasis ($P > 0.05$).

High *H19* expression is associated with poor prognosis of patients with GC. Kaplan–Meier analysis and log-rank test were used to evaluate the effects of *H19* expression and the clinicopathological characteristics on disease-free survival (DFS) and overall survival (OS). The results showed that patients in the high *H19* expression group had a higher recurrence rate (median DFS: 15 months) and much shorter overall survival (median OS: 18 months) than those in the low *H19* expression group (median DFS: 25months; median OS: 28 months; p = 0.007 and 0.001, respectively; Figure 2A, 2B). The 3-year DFS and OS were 34.8% and 32.5%, respectively, in the high *H19* expression group, and 43.7% and 52.8%, respectively in the low *H19* expression group. Univariate analyses of clinical variables considered as potential predictors of survival are shown in Table 2. The results revealed that *H19* expression, TNM stage and distant metastasis were associated with DFS, while invasion depth, regional lymph nodes, *H19* expression, TNM stage and distant metastasis were related to OS. Further analysis in a multivariate Cox proportional hazards model showed that *H19* expression, together with TNM stage, was strongly associated with DFS. *H19* expression was an independent prognostic indicator of DFS (hazard ratio [HR] = 1.287; 95% confidence interval [CI], 1.002–1.652; p = 0.048) in patients with GC (Table 2).

Observation of the diagnostic value of using *H19* as a marker. We observed whether *H19* could be used as a GC marker. We used corresponding adjacent non-tumorous tissues as a control to produce an ROC curve. The cutoff value was 4.615 (Δ Ct value). The area under the ROC curve was

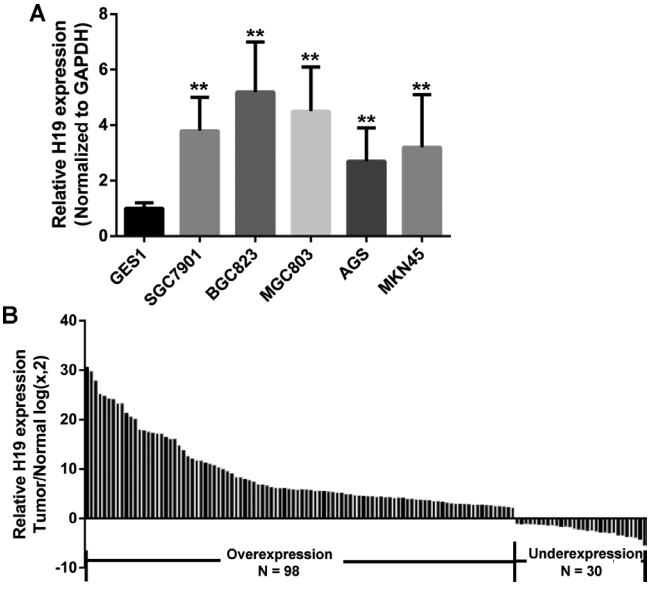

Figure 1. Relative expression of *H19* in GC cell lines and GC tissues A. Relative expression of *H19* in five GC cell lines (SGC7901, BGC823, MGC803, AGS and MKN45) and human normal gastric epithelial cell line (GES1) analyzed by quantitative RT-PCR. Experiments were performed in triplicate. Bars: SD (p<0.01). B. Relative expression of *H19* in GC tissues and adjacent normal tissues.**

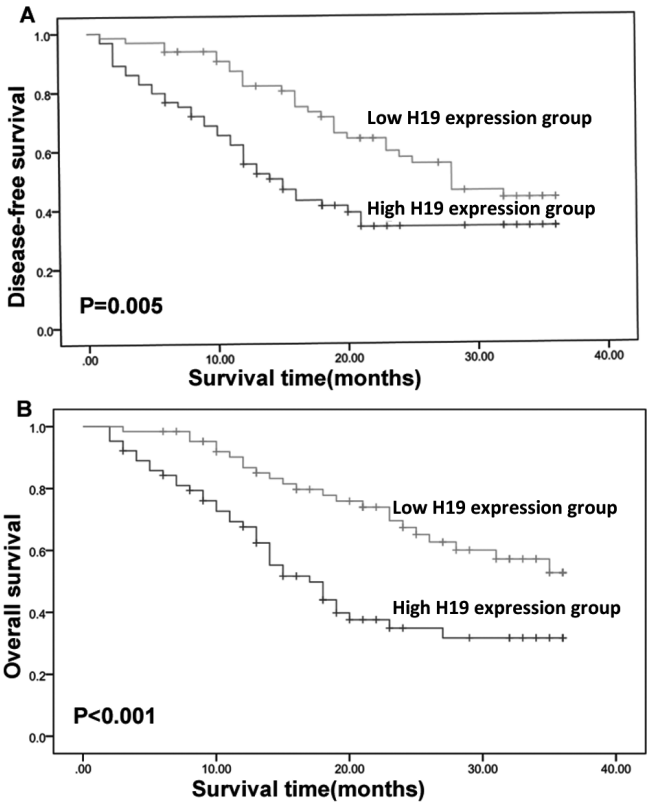

Figure 2. Kaplan–Meier overall survival curves of GC patients according to the level of *H19* expression A. Disease-free survival of patients with GC based on *H19* expression status (p < 0.001, log-rank) B. Overall survival of patients with GC based on *H19* expression status (p = 0.005, log-rank).

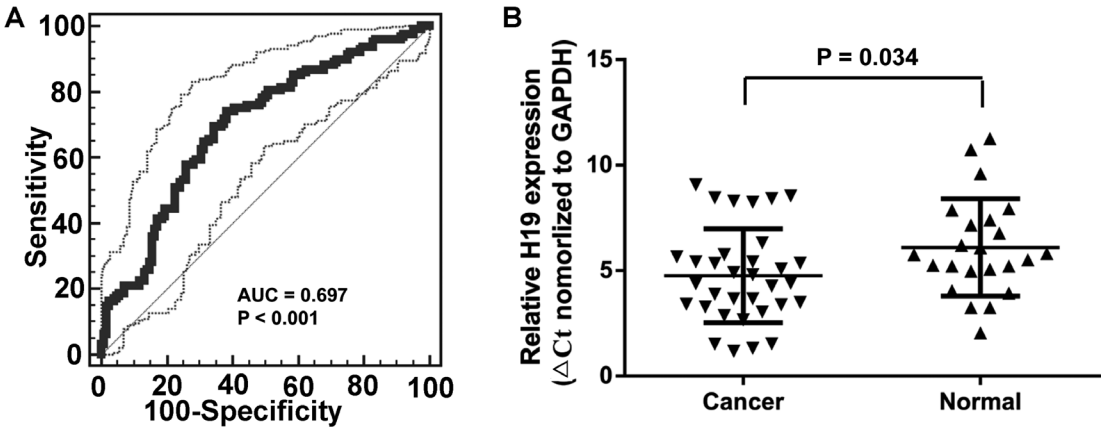

Figure 3. Diagnostic role of *H19* in GC A. Receiver operation characteristics (ROC) curve of using *H19* for differentiating GC tissues from normal tissues. The area under the ROC curve (AUC) is up to 0.697. B. Relative expression of *H19* from GC patients and normal subjects in gastric juice.

0.697; (95% CI = 0.636–0.752, $P < 0.001$; Fig. 3A). The sensitivity and specificity was 0.62 and 0.74, respectively. The Youden index of *H19* was 0.360.

Gastric juice is a simple and easy-to-obtain sample which can provide available information in the diagnosis of GC. To evaluate the diagnostic value of *H19*, the levels of gastric juice *H19* were detected in gastric juice between GC patients and normal cases. Interestingly, we found that *H19* levels in gastric juice from patients with GC were significantly higher than those from normal subjects (p = 0.034, Fig. 3B).

Knock down of *H19* represses GC cell migration and invasion in vitro. *H19* promoting GC cell proliferation has been well documented [24], we further evaluated the role of *H19* in cell migration and invasion. *H19* was depleted in BGC823 and MGC803 cells, which exhibit a higher expression of *H19*. The knockdown of *H19* in cells was confirmed by qPCR. (Fig. 4A). Subsequently, we observed the effect on cell migration and invasion. As shown in Fig. 4B, C, BGC823 and MGC803 cells, which have a naturally high *H19* expression, after knockdown of *H19*, showed markedly repressed migra-

Table 2. Univariate and multivariate Cox regression analyses *H19* for DFS or OS of patients in study cohort (n = 128).

Variables	DFS			OS		
	HR	95% CI	p value	HR	95% CI	p value
Univariate analysis					.	
Age(<50years vs. >50years)	0.825	0.512-1.329	0.428	0.909	0.550-1.502	0.708
Gender(male vs. female)	0.696	0.421-1.152	0.159	0.628	0.365-1.081	0.093
Location(Distal vs. Middle+ Proximal)	0.994	0.610-1.622	0.982	0.831	0.500-1.381	0.476
tumor size(>5cm vs. <5cm)	0.971	0.766-1.232	0.811	0.998	0.776-1.283	0.987
Histologic differentiation(Well+ Moderately vs. Poorly+ Undifferentiated)	1.381	0.842-2.263	0.201	1.418	0.840-2.395	0.192
Invasion depth(T3+T4 vs. T1+T2)	1.418	0.880-2.286	0.152	1.709	1.027-2.844	0.039*
TNM stage (III + IV vs. I+II)	2.269	1.406-3.662	0.001*	2.623	1.579-4.357	<0.001*
Lymphatic metastasis(No vs. Yes)	0.814	0.642-1.031	0.088	0.813	0.632-1.046	0.107
Regional lymph nodes(PN2+ PN3 vs. PN0+ PN1)	1.531	0.922-2.542	0.099	1.870	1.106-3.164	0.020*
Distant metastasis(No vs. Yes)	0.493	0.279-0.874	0.044*	0.488	0.270-0.883	0.018*
Expression of *H19* (High vs. Low)	1.397	1.099-1.777	0.006*	1.572	1.210-2.042	0.001*
Multivariate analysis						
TNM stage (I+II vs. III + IV)	1.519	1.058-2.181	0.023*	2.342	1.294-4.240	0.005*
Invasion depth(T3+T4 vs. T1+T2)				0.752	0.375-1.509	0.423
Regional lymph nodes(PN0+ PN1vs. PN2+ PN3)				0.779	0.363-1.674	0.522
Distant metastasis(No vs. Yes)	0.814	0.423-1.568	0.539	0.269	0.077-0.945	0.041*
Expression of *H19* (High vs. Low)	1.287	1.002-1.652	0.048*	1.959	0.966-3.973	0.062

*P < 0.05

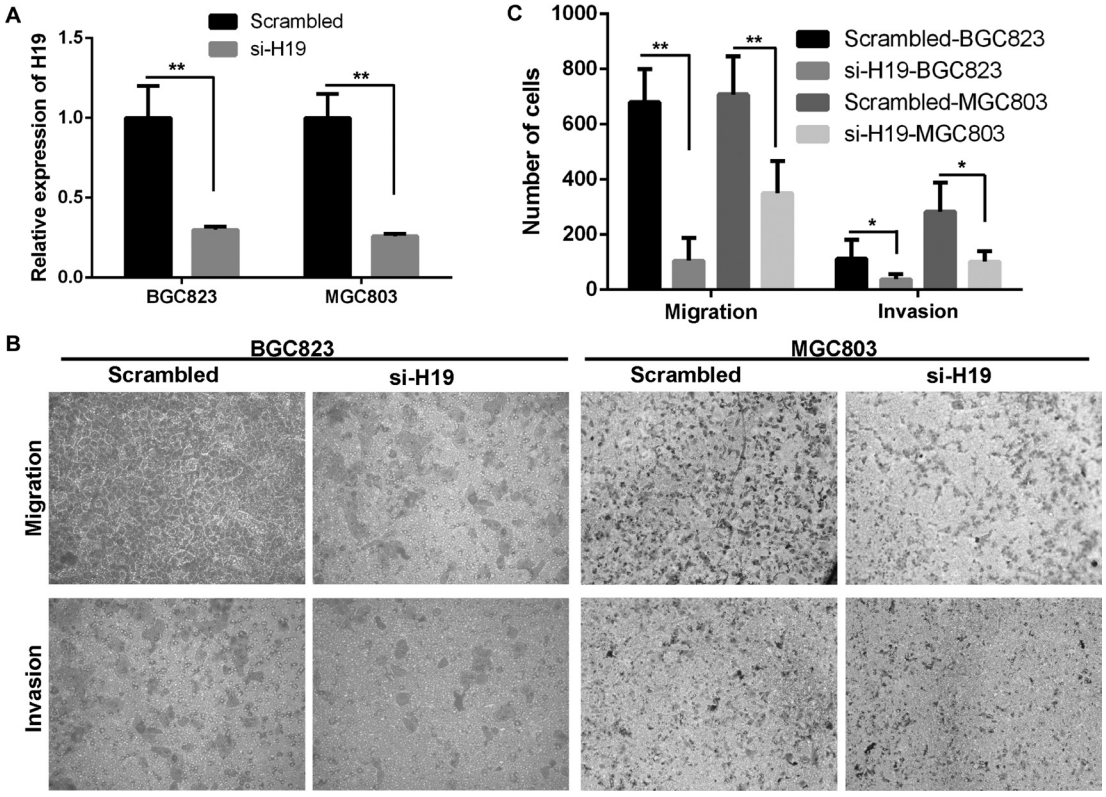

Figure 4. Knockdown of *H19* inhibits GC cell migration and invasion in vitro A. qPCR analysis of *H19* expression levels following the treatment of BGC823 and MGC803 cells with scrambled siRNA and si-*H19*. Experiments were performed in triplicate. Bars: SD; **p < 0.01. B, C. Transwell assays were used to investigate the changes in the migratory and invasive abilities of GC cells. Experiments were performed in triplicate. Bars: SD; *p < 0.05 andp < 0.01.**

tion and invasion ability ($p < 0.05$). These findings indicate that *H19* may be closely associated with invasion and migration of GC cell lines.

***H19* affects the levels of E-cadherin proteins.** To explore the molecular mechanisms by which *H19* contributes to the phenotypes of GC cells, we investigated potential targets involved in tumor invasion and metastasis. Epithelial-mesenchymal transition (EMT) has been identified to participate in cancer invasion and metastasis, so we conducted western blotting assays to detect the expression of EMT-induced markers (E-cadherin, N-cadherin and Vimentin) in cells down-expressing *H19*. Our findings showed that inhibited *H19* expression levels remarkably induced E-cadherin expression, but with insignificant altered of N-cadherin and Vimentin expression (Figure 5).

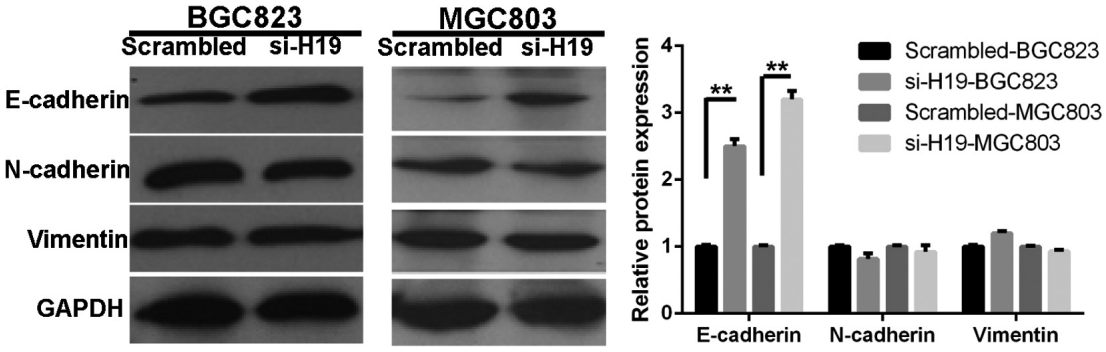

Figure 5. *H19* affects E-cadherin protein levels. Western blot analysis of E-cadherin, N-cadherin and Vimentin in *H19* knockdown expression GC cells and control cells. GAPDH protein was used as an internal control. **P<0.01

Discussion

H19 was the first lncRNA discovered [25]. Numerous studies indicate that *H19* may play a key role in tumorigenesis and could contribute to tumor progression and aggressiveness. *H19* overexpression has also been reported in various cancer tissues including breast, lung and esophageal cancers [19, 26, 27]. *H19* lncRNA mechanisms of action appear to be extremely diverse, acting at various levels. *H19* has been shown to guide chromatin modifying enzymes to specific loci. *H19* binds to and recruit the histone methyltransferase EZH2 at the E-cadherin promoter, leading to an increase in H3K27me3 repressive marks and to the silencing of the E-cadherin gene in bladder cancer [28]. *H19* is also illustrated by its dual interaction with miR pathways; it acts as miR sponge to sequester miR-106a [29]. *H19* serves as a precursor of miR-675 that post-translationally regulates a number of targets involved in cell tumorigenicity, including RUNX1 in GC [22]. However, the precise clinical significance in GC remains less understood.

In this study, we performed RT-qPCR to investigate whether *H19* was altered in 128 pairs of GC tissues and adjacent normal tissues. Results showed that the expression level of *H19* was increased in GC compared with that in adjacent normal specimens. Additionally, *H19* expression is markedly increased in GC cell lines compared with normal gastric epithelium cell line. An ROC curve was constructed and the results indicated that *H19* expression could better differentiate GC tissues from normal tissues. Aberrant expression of miRNA in gastric juice can be used as potential biomarkers for detecting GC [30]; however, there is little information on GC-specific lncRNAs. In the study, we found that gastric juice *H19* levels in GC patients were significantly higher than those of normal subjects. Recently, Zhou et al also demonstrated that plasma level of *H19* was increased in GC patients, and it may potentially be useful for cancer screening[31]. Compared with their study, our results have more obvious advantages in the diagnosis of GC, because gastric juice is present only in the stomach and easy to obtain. Our results provided evidence that expression level of *H19* was up-regulated in human GC, and this is the first time to characterize lncRNAs in gastric juice as diagnostic markers for GC.

To further determine the clinical significance of *H19*, the association between *H19* expression and clinicopathological parameters in GC tissues was analyzed. The results revealed that high *H19* expression was more frequently detected in tumors with deeper invasion depth, more lymphatic metastasis and advanced TNM stage. Additional, patients with a high expression of *H19* seemed to have shorter OS and DFS than patients with lower levels. Furthermore, multivariate Cox analysis showed that *H19* could serve as an independent prognostic biomarker. Since the clinicopathological parameters of depth of invasion, regional lymph nodes status and tumor stage represent partially the deterioration and progress of GC, *H19* might be involved in the tumorigenesis and progression of GC. *H19* promoting GC cell proliferation has been well documented [24], so we focus on the migration and invasion effects of *H19*. RNAi-mediated suppression of *H19* in BGC823 and MGC803 cells led to a significant inhibition of migration and invasion. Therefore, *H19* might serve to identify high-risk individual patients with GC who have higher risk of death and, thus, *H19* may represent a promising target for GC treatment.

To further document the molecular mechanism by which *H19* contributes to the migration and invasion of GC, we investigated potential target proteins involved in cell motility and matrix invasion. Here, loss of *H19* in GC cells led to a significant increase in E-cadherin protein levels. Decreased E-cadherin expression is one of the alterations that characterize the invasive phenotype, and the data support its role as a tumor suppressor gene [32]. Our findings indicate that lncRNA *H19* contributes to the GC cell migration and invasion maybe partly via regulating E-cadherin expression.

In conclusion, we demonstrated that *H19* was significantly up-regulated in GC tissues and some GC cell lines, and might be capable of distinguishing between cancerous and non-cancerous conditions by examining the expression of *H19* in tissues and gastric juices. Its level was associated with tumor progression and poor prognosis. This study revealed that *H19* may regulate the migration and invasion ability of GC cells partly through regulation of E-cadherin expression. These findings suggested that *H19* might be useful as a diagnostic and prognostic biomarker for GC and might be a possible target for gene therapy. However, larger clinical and prospective studies will need to be performed to confirm these preliminary results.

References

[1] MOORE MA, ATTASARA P, KHUHAPREMA T, LE TN, NGUYEN TH ET AL. Cancer epidemiology in mainland South-East Asia – past, present and future. Asian Pac J Cancer Prev 2010; 11 Suppl 2: 67–80.

[2] JEMAL A, SIEGEL R, XU J, WARD E. Cancer statistics, 2010. CA Cancer J Clin 2010; 60: 277–300. http://dx.doi.org/10.3322/caac.20073

[3] SAPARI NS, LOH M, VAITHILINGAM A, SOONG R. Clinical Potential of DNA Methylation in Gastric Cancer: A Meta-Analysis. Plos One 2012; 7. http://dx.doi.org/10.1371/journal.pone.0036275

[4] MILNE AN, CARNEIRO F, O'MORAIN C, OFFERHAUS GJA. Nature meets nurture: molecular genetics of gastric cancer. Human Genetics 2009; 126: 615–28. http://dx.doi.org/10.1007/s00439–009-0722-x

[5] PONTING CP, BELGARD TG. Transcribed dark matter: meaning or myth? Human Molecular Genetics 2010; 19: R162-R8. http://dx.doi.org/10.1093/hmg/ddq362

[6] HAUPTMAN N, GLAVAC D. Long Non-Coding RNA in Cancer. International Journal of Molecular Sciences 2013; 14: 4655–69. http://dx.doi.org/10.3390/ijms14034655

[7] MUERS M. RNA Genome-wide views of long non-coding RNAs. Nature Reviews Genetics 2011; 12. http://dx.doi.org/10.1038/nrg3088

[8] PONTING CP, OLIVER PL, REIK W. Evolution and Functions of Long Noncoding RNAs. Cell 2009; 136: 629–41. http://dx.doi.org/10.1016/j.cell.2009.02.006

[9] QI P, DU X. The long non-coding RNAs, a new cancer diagnostic and therapeutic gold mine. Modern Pathology 2013; 26: 155–65. http://dx.doi.org/10.1038/modpathol.2012.160

[10] RINN JL, KERTESZ M, WANG JK, SQUAZZO SL, XU X, BRUGMANN SA, et al. Functional demarcation of active and silent chromatin domains in human HOX loci by Noncoding RNAs. Cell 2007; 129: 1311–23. http://dx.doi.org/10.1016/j.cell.2007.05.022

[11] CALIN GA, LIU CG, FERRACIN M, HYSLOP T, SPIZZO R, SEVIGNANI C, et al. Ultraconserved regions encoding ncRNAs are, altered in human leukemias and carcinomas. Cancer Cell 2007; 12: 215–29. http://dx.doi.org/10.1016/j.ccr.2007.07.027

[12] LIN R, MAEDA S, LIU C, KARIN M, EDGINGTON TS. A large noncoding RNA is a marker for murine hepatocellular carcinomas and a spectrum of human carcinomas. Oncogene 2007; 26: 851–8. http://dx.doi.org/10.1038/sj.onc.1209846

[13] HIRATA H, HINODA Y, SHAHRYARI V, DENG GR, NAKAJIMA K, TABATABAI ZL, et al. Long Noncoding RNA MALAT1 Promotes Aggressive Renal Cell Carcinoma through Ezh2 and Interacts with miR-205. Cancer Research 2015; 75: 1322–31. http://dx.doi.org/10.1158/0008–5472.CAN-14–2931

[14] OKUGAWA Y, TOIYAMA Y, HUR K, TODEN S, SAIGUSA S et al. Metastasis-associated long non-coding RNA drives gastric cancer development and promotes peritoneal metastasis. Carcinogenesis 2014; 35: 2731–9. http://dx.doi.org/10.1093/carcin/bgu200

[15] SUN M, JIN FY, XIA R, KONG R, LI JH ET AL. Decreased expression of long noncoding RNA GAS5 indicates a poor prognosis and promotes cell proliferation in gastric cancer. Bmc Cancer 2014; 14. http://dx.doi.org/10.1186/1471–2407-14–319

[16] SUN M, XIA R, JIN FY, XU TP, LIU ZJ ET AL. Downregulated long noncoding RNA MEG3 is associated with poor prognosis and promotes cell proliferation in gastric cancer. Tumor Biology 2014; 35: 1065–73. http://dx.doi.org/10.1007/s13277–013-1142-z

[17] GABORY A, JAMMES H, DANDOLO L. The H19 locus: role of an imprinted non-coding RNA in growth and development. Bioessays 2010; 32: 473–80. http://dx.doi.org/10.1002/bies.200900170

[18] THORVALDSEN JL, DURAN KL, BARTOLOMEI MS. Deletion of the H19 differentially methylated domain results in loss of imprinted expression of H19 and Igf2. Genes Dev 1998; 12: 3693–702. http://dx.doi.org/10.1101/gad.12.23.3693

[19] KONDO M, SUZUKI H, UEDA R, OSADA H, TAKAGI K et al. Frequent loss of imprinting of the H19 gene is often associated with its overexpression in human lung cancers. Oncogene 1995; 10: 1193–8.

[20] BARSYTE-LOVEJOY D, LAU SK, BOUTROS PC, KHOSRAVI F, JURISICA I et al. The c-Myc oncogene directly induces the H19 noncoding RNA by allele-specific binding to potentiate tumorigenesis. Cancer Res 2006; 66: 5330–7. http://dx.doi.org/10.1158/0008–5472.CAN-06–0037

[21] ZHANG L, YANG F, YUAN JH, YUAN SX, ZHOU WP et al. Epigenetic activation of the MiR-200 family contributes to H19-mediated metastasis suppression in hepatocellular carcinoma. Carcinogenesis 2013; 34: 577–86. http://dx.doi.org/10.1093/carcin/bgs381

[22] ZHUANG M, GAO W, XU J, WANG P, SHU Y. The long non-coding RNA H19-derived miR-675 modulates human gastric cancer cell proliferation by targeting tumor suppressor RUNX1. Biochem Biophys Res Commun 2014; 448: 315–22. http://dx.doi.org/10.1016/j.bbrc.2013.12.126

[23] YANG F, BI J, XUE X, ZHENG L, ZHI K et al. Up-regulated long non-coding RNA H19 contributes to proliferation of gastric cancer cells. FEBS J 2012; 279: 3159–65. http://dx.doi.org/10.1111/j.1742–4658.2012.08694.x

[24] ZHANG EB, HAN L, YIN DD, KONG R, DE W, CHEN J. c-Myc-induced, long, noncoding H19 affects cell proliferation and predicts a poor prognosis in patients with gastric cancer. Med Oncol 2014; 31: 914. http://dx.doi.org/10.1007/s12032–014-0914–7

[25] BRANNAN CI, DEES EC, INGRAM RS, TILGHMAN SM. The product of the H19 gene may function as an RNA. Mol Cell Biol 1990; 10: 28–36. http://dx.doi.org/10.1128/MCB.10.1.28

[26] LOTTIN S, VERCOUTTER-EDOUART AS, ADRIAENSSENS E, CZESZAK X, LEMOINE J et al. Thioredoxin post-transcriptional regulation by H19 provides a new function to mRNA-like non-coding RNA. Oncogene 2002; 21: 1625–31. http://dx.doi.org/10.1038/sj.onc.1205233

[27] HIBI K, NAKAMURA H, HIRAI A, FUJIKAKE Y, KASAI Y, AKIYAMA S, et al. Loss of H19 imprinting in esophageal cancer. Cancer Res 1996; 56: 480–2.

[28] LUO M, LI Z, WANG W, ZENG Y, LIU Z, QIU J. Long non-coding RNA H19 increases bladder cancer metastasis by associating with EZH2 and inhibiting E-cadherin expression. Cancer Lett 2013; 333: 213–21. http://dx.doi.org/10.1016/j.canlet.2013.01.033

[29] IMIG J, BRUNSCHWEIGER A, BRUMMER A, GUENNEWIG B, MITTAL N et al. miR-CLIP capture of a miRNA targetome uncovers a lincRNA H19-miR-106a interaction. Nat Chem Biol 2015; 11: 107–14. http://dx.doi.org/10.1038/nchembio.1713

[30] CUI L, ZHANG X, YE G, ZHENG T, SONG H, DENG H, et al. Gastric juice MicroRNAs as potential biomarkers for the screening of gastric cancer. Cancer 2013; 119: 1618–26. http://dx.doi.org/10.1002/cncr.27903

[31] ZHOU X, YIN C, DANG Y, YE F, ZHANG G. Identification of the long non-coding RNA H19 in plasma as a novel biomarker for diagnosis of gastric cancer. Sci Rep 2015; 5: 11516. http://dx.doi.org/10.1038/srep11516

[32] GAMALLO C, PALACIOS J, SUAREZ A, PIZARRO A, NAVARRO P et al. Correlation of E-cadherin expression with differentiation grade and histological type in breast carcinoma. The American journal of pathology 1993; 142: 987–93.